Multimedia Tools and Applications (2021) 80:4203–4235
https://doi.org/10.1007/s11042-020-09727-3

Vision based inspection system for leather surface defect detection using fast convergence particle swarm optimization ensemble classifier approach

Malathy Jawahar[1,2] · N. K. Chandra Babu[1,2] · K. Vani[3] · L. Jani Anbarasi[4] · S. Geetha[4]

Received: 19 October 2019 / Revised: 11 July 2020 / Accepted: 25 August 2020 /
Published online: 28 September 2020
© Springer Science+Business Media, LLC, part of Springer Nature 2020

Abstract
Surface defect inspection plays a vital role in leather manufacturing. Current practice involves an expert to inspect each piece of leather individually and detect defects manually. However, such a manual inspection is highly subjective and varies quite considerably from one assorter to another. Computer vision system for natural material like leather is a challenging research problem. This study describes the application of computer vision system to capture leather surface images and use of a novel Fast Convergence Particle Swarm Optimization (FCPSO) algorithm on a set of handcrafted texture features viz., GLCM and classified using supervised classifiers viz., Multi Layer Perceptron (MLP), Decision Tree (DT), SVM, Naïve Bayes, K-Nearest Neighbors (KNN) and Random Forest (RF). FCPSO using modified fitness function by selective band Shannon entropy is implemented to segment industrial leather images. Segmentation efficiency of the proposed FCPSO algorithm is evaluated and its performance is compared with other optimization algorithms. Efficiency of the segmentation algorithms is evaluated using performance measures such as average difference (AD), Area Error Rate (AER), Edge-based structural similarity index (ESSIM), F-Score, Normalized correlation coefficient (NK), Overlap Error (OE), structural content (SC), Structural similarity index (SSIM) and Zijdenbos similarity index (ZSI). Correlation of the segmented area using FCPSO with the experts' ground truth is found to be high with R value of 0.84. Feature extraction is carried out using GLCM texture features and the most prominent features were selected using statistical t-test and correlation coefficient. Experimental results showed encouraging results for random forest classifier confirming the potential of the proposed system for automatic leather defect classification.

Keywords Image analysis · Leather surface defect detection, segmentation · Fast convergence particle swarm optimization · Ensemble classifier

✉ Malathy Jawahar
malathy.jawahar@gmail.com

Extended author information available on the last page of the article

1 Introduction

Hides and skins, raw material for the leather industry, being natural material suffer from many defects or surface blemishes, which downgrade the quality of leathers made from them. Defects on hides and skins are broadly classified as ante-mortem (defects caused before the death of animal) and post-mortem (defects caused after the death of the animal). Apart from these, defects can manifest on leathers due to faulty leather processing methods. Common defects found in leather are brand marks, tick marks, pox marks, insect bite,wounds,scratches,growth marks, flay cuts, veininess, wrinkles, fat folds, salt stain, lime blast, chrome or dye patches, drawn grain, open cuts, pin hole damage etc.

Quality inspection for grading is an important step in assessing the usable area of leathers. Each piece of leather is graded based on its effective cutting value, which is decided taking into consideration the number, size and location of surface defects. Leather price varies according to the effective cutting value and hence grading is done with great care by experienced assorters. But visual inspection is tediously repetitive, and hence fatigue can lead to defects passing unnoticed, leading to inaccuracy and inconsistency. Scientific advances made in the area of digital image processing (DIP) can be profitably exploited for developing an accurate and objective automatic leather defect inspection system [3, 26] . The first step in that direction would be to device a suitable image processing method for the purpose of defect identification and classification. Natural leather surface itself has an inherent texture due to hair pore arrangements and other natural grain indentations, which vary quite considerably from one type of leather to another, and hence separation of defects from sucha complex background is a quite challenging task. Several researchers have developed methods for leather defect classification based on computer vision. Many segmentation methods have been proposed over the years for medical [2, 32, 58] and natural images [10, 20, 44, 56, 72]. A contour segmentation [4, 9] using heuristic rule was applied for leather defect segmentation. Otsu thresholding, one of the simple and robust segmentation technique has been used by many researchers and applied it for leather images [71]**.** Segmentation of leather image based on minimum error threshold [25], mathematical morphology [65], structural image segmentation [36], histogram distribution [68], multi-resolution pyramid structure [41], node linking edges' pyramid [42], crude syntactic segmentation [52], multiband image segmentation [12] and schemes that involved both threshold and morphological based segmentation [38, 39], auto adaptive edge detection [31] methods were proposed by various researchers. To simplify the segmentation process for leathers, some researchers have resorted to have manual marking of defects and classifying the regions using image processing [24, 47, 51, 64]. Quadtree decomposition scheme to partition leather images into homogeneous blocks using thresholding has also been proposed [36]. Wavelet based segmentation and segmentation using Gabor filtertuned at different scales for various defects [5–7, 22, 23, 44, 60] were also attempted for leather defect segmentation. To solve optimisation problems, Particle Swarm Optimisation (PSO) algorithm was introduced by Kennedy & Eberhart [33]. Many researchers have attempted to address the problem of finding optimal threshold values for segmenting images using biologically inspired algorithms [16, 18, 37, 43, 45, 46, 54, 55, 58] . Segmentation using deep learning methods are being practiced in manufacturing industries [14, 53]. Leather being natural material, many of the defects are found to be dispersed in nature and varied multiple type of defects occur together. Hence, generating large number of annotated ground truth images for training deep learning [35] is challenging. Segmentation methods for leather defect images are often evaluated by employing still leather images of small window size or reduced number of

samples, and hence very far from industrial operating conditions. This study mainly focuses on developing best performing PSO variant in terms of time when applied for industrial leather images.

In its beginnings, defect detection in leather images was greatly influenced by the choice of suitable pre-defined features and the subsequent use of traditional machine learning classifiers. Indeed, this feature identification and extraction process is arguably the most significant phase in the defect detection procedure where the main job is to describe the defective leather characteristics in a more distinctive way. The feature extration process takes image pixels as inputs and produces as output - a feature vector 'FV' which encodes a specific aspect of the image like shape, texture, color, etc. These feature vectors are used to build a classifier by training on the underlying patterns denoted by the extracted feature vectors. Texture perception has a very substantial role to play in human visual system of recognition. Similarities and dissimilarities in intensity variations are described well by texture feature. The most successful and highly used hand-crafted texture features in the literature are Haralick features [21] derived from Gray Level Co-occurrence Matrix (GLCM), which extract the local patterns in the image and count their distribution across the entire image. They provide a good discriminative encoding of the textural and gradient based information, in the form of feature values. In this work, we consider the top performing representative Haralick features from GLCM values and investigate their discriminative power and robustness.

Currently, deep learning methods [17, 40] are advancing at a rapid pace and they have become a promosing data-driven learning strategy for numerous computer vision tasks. They perform feature engineering to yield natural-features from images, by combining both the traditional steps: feature extraction and classification, together as an end-to-end paradigm. Convolutional Neural Network (CNN) is one such typical deep learning model for feature engineering. CNN is constructed by stacking multiple neural network layers on top of each other. They possess a set of filters that figure out the discriminative features from the images fed as inputs to CNN. The lower layers of the CNN contains filters which learn more generic characteristics from the images, like edges and corners, whereas the higher layers contain filters which use the low level features and learn more abstract and complex characteristics, which will differentiate images of one class from the images of other class. The CNNs directly operate on the raw image pixels and thus automatically learn the discriminative features from the images, during the CNN training procedure. With this situation, the CNN is open and free to utilize features from all the levels (low and high) and thus learn better semantic information from the given images. Further, a deep CNN training procedure has an additional advantage - i.e., refining the input data representation to match the requirement of a particular problem. Additionally, the feature engineering process led by the CNN training procedure, is encountered with the high adaptiveness of deep learning paradigms.

Deep learning doesn't work so well with small data. The CNN models achieving superior performance in the latest research are often trained over hundreds of thousands and even millions of samples. In order to learn better visual representations, and arrive at good discriminating features, and thereby subsequently improve the defect detection performance, deep CNNs do require huge labeled datasets [62], maybe even in the order of ten thousands. The derived features prove to be effective only when the training dataset is voluminous and contain considerable representations for images in all classes. The model performance is better, when we have more labelled data. Since in the deep learning paradigm, data is the most valuable resource and the leather imageset faces the issue of only less unlabelled images.

Nevertheless, there are practical situations, while solving real-world problems like ours, leather imageset, where the availability of such labelled training data is constrained and limited and large datasets do not exist. In such cases, the use of deep learning methods is an infeasible option, and conventional feature extraction and classification techniques will become the proper solution. Unfortunately for this leather defect detection applications, such large datasets are not readily available and is an expensive and time consuming to acquire. With the available smaller datasets of leather images, classical ML algorithms such as regressions, random forest, and SVM often outperform deep networks.

Furthermore, deep networks are not easily comprehended. Deep networks are kind of a "black box" wherein it is not possible to fully understand the "inside" of deep networks. Their predictive power is high but they come with low comprehensive ability. ie., the interpretation ability. Hyper-parameters and network design are also quite a challenging due to the week understanding of the theoretical foundation. There has been a lot of recent tools like saliency maps and activation differences that work great for some domains like object detection. Unfortunately this knowledge does not transfer completely to all applications, in the same performance level. These tools are majorly designed to ensure that the network model is not overfit on the dataset or is not focusing on certain features that are spurious. Furthermore, it is still difficult to comprehend per-feature importance towards the overall decision made by the deep net.

Contrarily, classical ML algorithms such as SVM, Random Forests etc., come with comprehensive ability and are understandable due to the direct feature engineering process. Further, hyper-parameters tuning and the model designs modifications are made straightforward since there is a good understanding of the underlying algorithms and the data. These are particularly important when the results of the model have to be translated and delivered to the domain platform, where-in sometimes there are non-technical audience like leather defect detection task.

This leather defect detection problem is one such real world problem, where the availability of huge labelled imageset is a constraint and an understanding of how the detection is arrived proves to be more helpful [27, 28]. Hence, in the present investigation, an attempt has been made to derive Fast Convergence Particle Swarm Optimization (FCPSO) algorithm based on multi-thresholding to determine optimal threshold level for segmenting complex leather surface image and was compared with various segmentation algorithms. Effectiveness of the segmented area by FCPSO algorithm and PSO variants, GA were validated in comparison with manually segmented area by the experts using correlation (R value). Haralick features extracted from co-occurrence matrices were computed from segmented leather images. Feature Selection based on correlation coefficient and t-test were carried out. Supervised Classification using Multi Layer Perceptron (MLP), Decision Tree (DT), SVM, Naïve Bayes, KNN and Random Forest (RF) classifiers were used to classify the defective and non-defective leather regions [26]. Main contributions of the proposed method are

i. FCPSO algorithm to segment the leather defects from the complex background.
ii. Analyzing the performance of various PSO segmentation algorithm using statistical measures.
iii. Feature Selection based on Correlation coefficient and t-test for choosing the most prominent GLCM texture features.
iv. Classification and performance validation of various supervised based on the discriminant feature vector.

2 Materials and methods

2.1 Image acquisition

Leather images used in this study were captured using a specially designed industrial leather image acquisition system. Leather sample was conveyed using a feed and a delivery roller. Sony industrial CCD colour camera with USB 3.0 interface was mounted on a horizontally moving carriage. As the leather is conveyed, the carriage moves the camera horizontally from left to and right and images were captured. Number of frames captured for each leather sample varies considerably depending on the size of the leather and each acquired leather image was 1600×1200 pixels. Database comprising 115 defective and 85 non-defective image frames were developed for use in the study. Ground-truth (GT) images were manually segmented by experienced leather assorters. Out of these, 140 samples images were used for the training and remaining 60 samples for testing. Image processing techniques proposed in this study were programmed in Scilab environment.

2.2 Image preprocessing

Leather being a natural material has large variations of gray level intensities due to the inherent texture and natural grain indentations. Wiener filter provides an optimal tradeoff in restoring the effects of unequal brightness and contrast as well as noise smoothing in the leather images. The preprocessed leather images were qualitatively analyzed by MSE (Eq. 1) and PSNR (Eq. 2) values and further subjected to segmentation using FCPSO.

$$MSE = \frac{1}{M \times N} \sum_{i=1}^{M} \sum_{j=1}^{N} \left(C_{ij} - S_{ij}\right)^2 \tag{1}$$

$$\mathrm{PSNR} = 10 \times 10 \log \left[\frac{255^2}{\mathrm{MSE}}\right] \mathrm{dB} \tag{2}$$

2.3 Image segmentation

Image segmentation assign a label to each pixel in the image such that pixels withthe same label share certain visual characteristics. Elliminating the bachground and extracting the defective regions is the Region of Interest. texture analysis, histogram thresholding, clustering based methods and region based split and merging methods were the various image segmentation algorithms. The exhaustive search method based on the Otsu criterion is simple, but it has a disadvantage that it is computationally expensive. Alternative to Ostu, various biologically inspired algorithms were explored in image segmentation. The Particle Swarm Optimization (PSO) is a machine-learning technique loosely inspired by birds flocking in search of food. It basically consists of a number of particles that collectively move in the search space. For better modeling of natural selection, PSO variants like DPSO, FODPSO, and evolving optimized PSO [59] have better convergence rate. A parallel PSO was presented for three different communication strategies by [11, 19] . Optimizing th topology design of distributed local area network is analysed by Salman and Andries [13, 15, 34] using fuzzy PSO where fuzzy aggregation operator is used to aggregate the objective [30]. The coverage problem in

wireless sensor is improved using particle swarm optimization based on dynamic acceleration coefficient by Teng et al. [63]. Summarily, all of the existing PSO methods mentioned above possess respective advantages like fast convergence, information sharing and robustness and adversities like local optimum, premature convergence and curse of dimensionality etc.

2.3.1 Proposed fast convergence particle swarm optimization segmentation algorithm

In this study, a modified Fast ConvergenceParticle Swarm Optimization algorithm was adopted for segmenting defective regions in the complex leather images. Swarm intelligence is a useful model for adaptive systems. Let I denote the leather image of size M x Nrepresented and the intensity value of the image as individual particleswith gray levels ranging from 0 to 255.Each particle of the swarm represents a possible solution. PSO is to learn from the particles' individual experience and also from its neighborhood experience. Based on the probability intensity distribution, particles movestochastically according to its position(X_k^i) and velocity (V_k^i) in the direction of its local remembered individual particle position (l_k^i) and the whole swarm's global best remembered swarm position (g_k^i).Success of the particle was evaluated by the fitness function. Each particle in the swarm is iteratively updated according to the particle position, velocity and past best position.

Velocity and Position of the individual particle wascalculated as given in equations [3, 4],

$$V_{k+1}^i = WV_k^i + \rho_1 r_1 \left(l_k^i - X_k^i\right) + \rho_2 r_2 \left(g_k^i - X_k^i\right) \tag{3}$$

$$X_{k+1}^i = X_k^i + V_{k+1}^i \tag{4}$$

The new velocity is determined using inertia influence (W), and learning factors ρ_1, ρ_2. Random vectors (r_1, r_2) are generally assigned a random values ranging between 0 and 1. Learning factor $\rho 1$ adjusts the particle movement towards its local best position and $\rho 2$ adjust the particle towards the global best. Second term $\rho_2 r_2 \left(l_k^i - X_k^i\right)$ in Eq. 3 is said to be individual cognitive component is a linear attraction towards the individual best position found by the given particle and the corresponding best fitness value is represented as pbest and is referred to as memory or self-knowledge. $\rho_1 r_1 \left(g_k^i - X_k^i\right)$ in Eq. 3 is said to be a social cognitive component is a linear attraction towards the best position found by any particle at which the best fitness in a neighborhood so far has been achieved. The corresponding best fitness is represented as gbest and as cooperation or social knowledge. At the beginning of the iteration, particles needs to be initialized in such a way that they are distributed as evenly as possible in the problem search space. Similarly, asmallself-cognitive component and a large social cognitive component would facilitate the convergence as well as to prevent the explosion of the swarm.

In conventional PSO, inertia influence (W) would be assigned a constant value slightly less than 1 for all the iterations. Inertia is the parameter that balances and controls exploration of the search. A high inertia value at the beginning of the iteration allows the particle to move freely to find the global optimum and after reaching the optimal region, inertia value needs to be reduced in order to narrow down the search thus shifting from the exploratory approach to exploitative approach. Hence, a dynamically changing inertia will facilitate faster convergence of the particles [29, 48, 69, 70]. As the particle in the swarm was updated, for each iteration a new modified dynamically changing inertia (W) with value strictly less than 1 was computed

(Eq. 5). The coefficient decreases as the number of iterations increases accordingly ensures the particles to escape from local minima and leads to faster convergence.

$$
\begin{aligned}
&|W| = |\frac{V_{k+1}^{i}}{V_k} + \frac{\rho_1 r_1 \left(g_k^i - X_k^i\right)}{V_k} + \frac{\rho_2 r_2 \left(l_k^i - X_k^i\right)}{V_k}| \leq k \\
&where\, |W| \leq 1 \\
&|\frac{V_{k+1}^{i}}{V_k}| + |\frac{\rho_1 r_1 \left(g_k^i - X_k^i\right)}{V_k}| + |\frac{\rho_2 r_2 \left(l_k^i - X_k^i\right)}{V_k}| \prec k \\
&(i.e)\ |\frac{V_{k+1}^{i}}{V_k}| \prec k, \quad |V_{k+1}^{i}| \prec k * V_k \\
&\quad |\frac{\rho_1 r_1 \left(g_k^i - X_k^i\right)}{V_k}| \prec k, \ |\rho_1 r_1 \left(g_k^i - X_k^i\right)| \prec k * V_k \\
&\quad |\frac{\rho_2 r_2 \left(l_k^i - X_k^i\right)}{V_k}| \prec k, \quad |\rho_2 r_2 \left(l_k^i - X_k^i\right)| \prec k * V_k
\end{aligned}
\tag{5}
$$

Selective band entropy wasperformed to evaluate the score of each position. Let N_i^j be the number of occurrence of O_i and its frequency Of_i^j in each category$C_j$was computed between $L_{\min}$and $L_{\max}$.

The values of $L_{\min}$ *and* $L_{\max}$were computed using the normal function f(x) as given in Eq. (6) by analyzing the distribution of the various defect images, where the minimum and the maximum distribution are considered for better randomness.

$$
f(x) = \left\{ \begin{matrix} {}^{(x-Mean)}\big/_{SD} & (100 \leq x \leq 170) \\ 0 \quad Otherwise & \end{matrix} \right\} \tag{6}
$$

where ‘x’ refers to the gray level intensity value ranging from 100 to 170 lies in the normal curve and for non-defects the line lies in the asymptotic curve.

The fitness function F_{fc} was computed using Shannon entropy [57] for the computed frequency occurrence within the range as given in Eq. 7.

$$
\begin{aligned}
F_{fc} &= -\sum_{j=L_{\min}}^{L} {}^{\max}\left(Of_i^j\right) \log\left(Of_i^j\right) \\
Of_i^j &= \frac{N_i^j}{\sum_{j=L_{\min}}^{L_{\max}} N_i^j}
\end{aligned}
\tag{7}
$$

The proposed FCPSO algorithm (Fig. 5) initialize the particles and computes fitness value of each particle using selective band entropy (Eq. 7). pbest is updated when the current fitness value is better than previous assumed pbest value. Gbest for each particle is determined by choosing the particle with the best fitness value of all neighbours. For each particle, velocity is updated (Eq. 3) using modified inertia influence (W) which changes dynamically for each iteration for each iteration (Eq. 5) rather than fixed value as in conventional PSO. Likewise particle position is also updated (Eq. 4). The process continues till the maximum iteration is attained.

2.3.2 Validation measure

The FCPSO segmented region was validated with the manually segmented defect region by the expert (Ground Truth - GT). Performance measures such as Average difference (AD), Area Error Rate (AER), Edge-based structural similarity index (ESSIM), Normalized correlation coefficient (NK), Overlap Error (OE), Structural content (SC), Structural similarity index (SSIM) and Zijdenbos Similarity Index (ZSI) [2, 32] were performed to quantify the accuracy of the FCPSO algorithm as given in Eqs. 8–16.

$$AD = \sum_{J=1}^{M}\sum_{K=1}^{N}\left[X(j,k) - \widehat{X}(j,k)\right] \Big/ MN \tag{8}$$

$$SC = \sum_{j=1}^{M}\sum_{K=1}^{N}\left[X(j,k)^2\right] \Big/ \sum_{j=1}^{M}\sum_{K=1}^{N}\left[\widehat{X}(j,k)^2\right] \tag{9}$$

$$IF = 1 - \sum_{j=1}^{M}\sum_{K=1}^{N}\left[X(j,k) - \widehat{X}(j,k)^2\right] \Big/ \sum_{j=1}^{M}\sum_{K=1}^{N}\left[X(j,k)^2\right] \tag{10}$$

$$NK = 1 - \sum_{j=1}^{M}\sum_{K=1}^{N}\left[X(j,k)\,\widehat{X}(j,k)^2\right] \Big/ \sum_{j=1}^{M}\sum_{K=1}^{N}\left[X(j,k)^2\right] \tag{11}$$

$$SSIM = l(x,y)^{\alpha}, c(x,y)^{\beta}, s(x,y)^{\gamma} \tag{12}$$

$$ESSIM = l(x,y)^{\alpha}, c(x,y)^{\beta}, e(x,y)^{\gamma} \tag{13}$$

Where $X(j,k)$ *and* $X(j,k)$ refers to the FCPSO segmented region and manual segmentation region, M,N refers to the size of the image, $l(x,y)$, $c(x,y)$, $s(x,y)$, $e(x,y)$ refers to the luminance, contrast, structural and edge component of the FCPSO segmented region and manual segmentation region and R_p represents the segmented region using FCPSO and R_m corresponds to manual segmented region.

$$ZSI = \frac{2*(M \cap P)}{|M| + |P|} \tag{14}$$

$$\mathrm{AER} = \frac{(M \cup P) - (M \cap P)}{M} \tag{15}$$

$$\mathrm{OE} = \left[1 - \left(\frac{M \cap P}{M \cup P}\right)\right] * 10 \tag{16}$$

where 'M' represents the manually segmented region by the experts and 'P'represents the defect region segmented by the proposed FCPSO algorithm.

Error between the FCPSO segmented region and manually segmented region is represented by AER and OE. Segmentation results are considered to be accurate when Edge-based structural similarity index (ESSIM), Normalized correlation coefficient (NK), Structural content (SC), Structural similarity index (SSIM), F-score value and ZSI values are ideally closer to 1.0 whereas Average difference (AD), AER and OE values are closer to zero. Image segmentation using PSO, DPSO, FODPSO and GA were performed to segment the defect regions and was compared with proposed FCPSO algorithm.

2.4 Feature extraction

The feature vector set was formed using second order texture information by constructing Gray Level Co-occurrence (GLCM) matrix from images. GLCM involves the estimation of probability density function P (i, j /Δx,Δy) where i and j indicate the gray level of two pixels and Δx and Δy denotes spacing between the pixels in x and y dimensions respectively [1, 3, 65–67]. In this study, co-occurrence matrices were calculated for 4 offset angles of 0°, 45°, 90° and 135° keeping the offset distance 'd' as 1. For example, contrast feature which represents the local abnormality present in the image was computed with d = 1 and offset angles (0,45,90,135) which results in four features (con_0, con_45, con_90, con_135). The average of these four features (con_0, con_45, con_90, con_135) was dervied as Contrast – Average (F2). Similarly, the difference between maximum (con_0, con_45, con_90, con_135) and minimum (con_0, con_45, con_90, con_135) was dervied as Contrast – Range (F22). Table 4 lists the 40 texture features namely the 20 average and 20 range features used in this study.

Homogeneity of the leather surface was showed in Angular second moment (ASM), Inverse Difference Moment (IDM) features. Good leather surface had homogeneous texture and exhibited higher ASM and IDM values whereas non homogeneous defective leather image revealed smaller values. Local intensity variations present in the leather image was indicated in Contrast feature. Gray level linear dependencies in the image were displayed as Correlation feature. Most of the leather defective regions had a coarse texture with high randomness of the gray level distribution and was captured in Entropy, Variance. Even though all 40 features describe the textural characteristics of the image, it is difficult to relate each of these features to image-specific textural characteristic.

2.5 Supervised classification

Classification is defined as a process of finding a set of attributes to distinguish between classes of data for the purpose of predicting the class of objects, whose class label is unknown. Decision boundary generated by the classifier seperates the elements in the feature space into two or more sets of classes. Different Classifers arrives at a unique decision boundary using its specific working process. The Supervised classfiers like Neural Network (NN), Decision Tree (DT), SVM, Naïve Bayes, KNN and the proposed Random Forest (RF) classifiers were analysed for distinguishing two classes of leather features [26, 50].

The Random Forest (RF) classifier is a combination of multiple decision tree proposed by Breiman [8]. Each tree can be viewed as an individual classifier and casts a unit vote for the

final classification of the input feature set. Random Forest splits each node using randomly chosen best subset of features. Feature variable importance measure, prediction error on the out-of-bag portion for each tree was computed. The same computation was carried out after permuting each feature variable. Mean and normalized standard deviation was computed. Splitting of tree stops when standard deviation of the difference in feature variable equal to 0.

Random forest uses the gini index to measure the node impurity. It is the measure most commonly chosen for classification-type problems. Gini(T) is defined as

$$Gini(T) = 1 - \sum_{j=1}^{n} P_j^2 \tag{17}$$

Where P_j represents relative frequency of dataset T with n classes.

The work flow of random forest algorithm is illustrated in Fig. 6.

To evaluate the proposed classifier accuracy as well as its generalization capability, feature vectors were randomly shuffled into 10 different groups. Each group contained 70% of the data for training and the remaining 30% for validation. Validation accuracy was averaged across all 10 trials. Performance measurements such as Sensitivity, Specificity, and Precision /Positive Predictive Value (PPV), Recall / Negative Predictive Value (NPV) and F1 score were also computed from the confusion matrix [61, 73].

3 Results and discussion

In this study, leather images were obtained using specially designed industrial image acquisition system (see Fig.1). Fast Convergence Particle Swarm Optimization (FCPSO) was used in segmentation of leather images which were preprocessed using wiener filter. Feature extraction was done using Haralick's texture feature method that represents the second order statistical texture features. Correlation coefficient was used to select the optimal features. Classification was carried out using random forest to solve the leather defect detection. The proposed methodology is described in Fig. 2.

It can be observed from Fig. 3 that normal leather images have very smooth texture, and are highly homogeneous in nature compared to the defective leather images which have rough and coarse texture with deep patches. This shows that the defective region pattern was different and not uniform. These pattern changes were analyzed by segmentation and feature analysis.

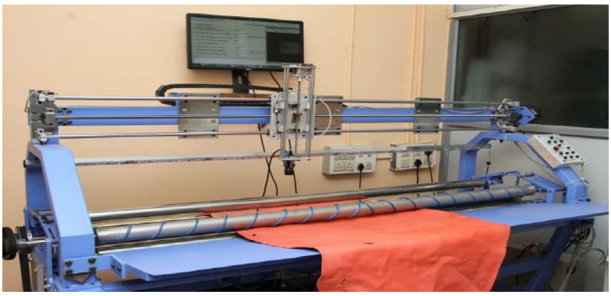

Fig. 1 Leather image acquisition system

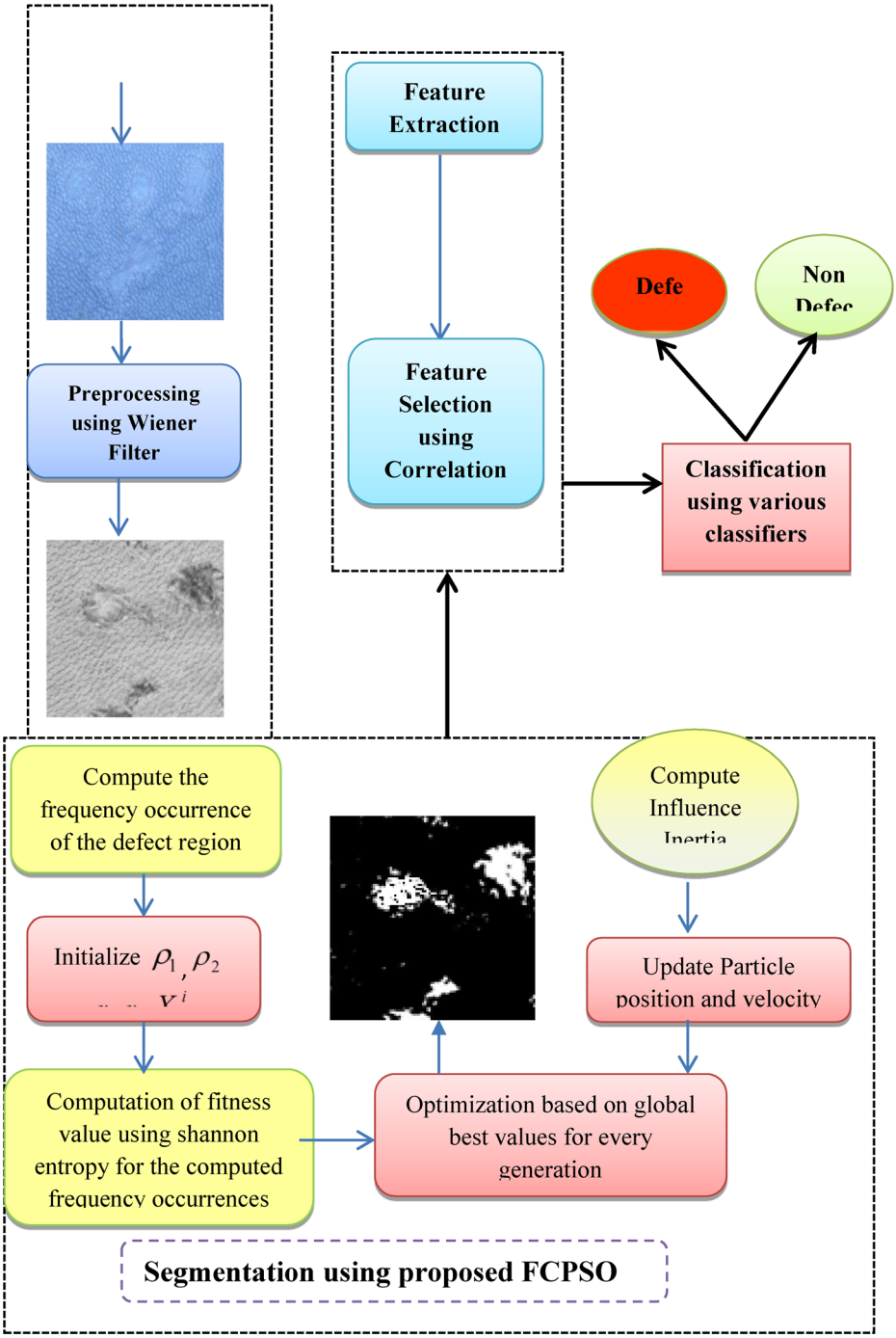

Fig. 2 Block diagram of proposed FCPSO defect detection methodology

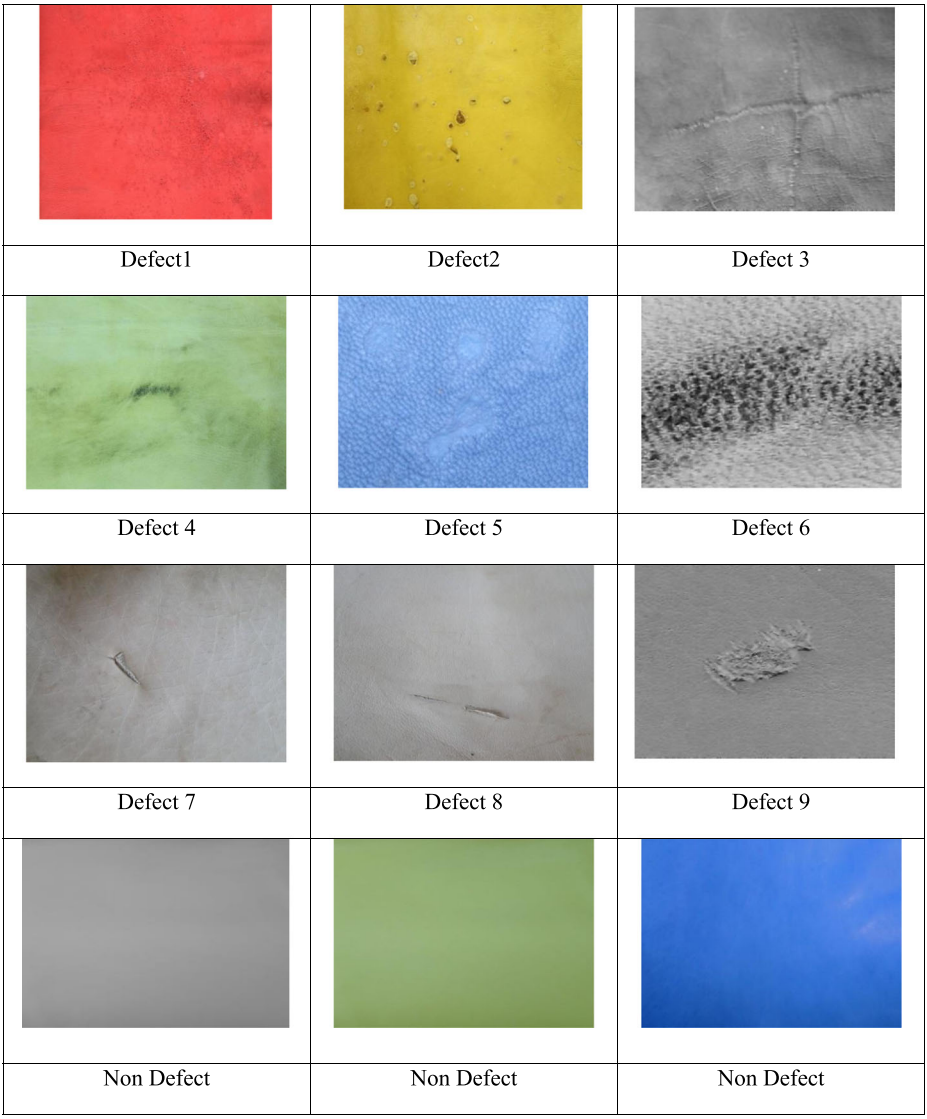

Fig. 3 Representative original defective leather Images

The enhanced images pre-processed using Wiener filter are depicted in Fig. 4. The pre-processed image was also examined visually. The qualitative analysis of the preprocessed image was found to have a low MSE (22.86) and a high PSNR value (71.16).

In conventional PSO, an exhaustive search with constant values for W is used for finding the optimal threshold values. To find an optimum threshold level, the number of iterations increases resulting in increased computation time. In the proposed FCPSO (Fig. 5), for each iteration, a new random inertia influence (W), which was strictly less than 1(Eq. 6), was computed for all the particles in the swarm. The new inertia influence(W) avoids the drifting behavior of particles around false solutions (Fig. 6). Figure 7 histogram distribution shows that the defective region lies in the range of 100 to 170. Selective band entropy based fitness

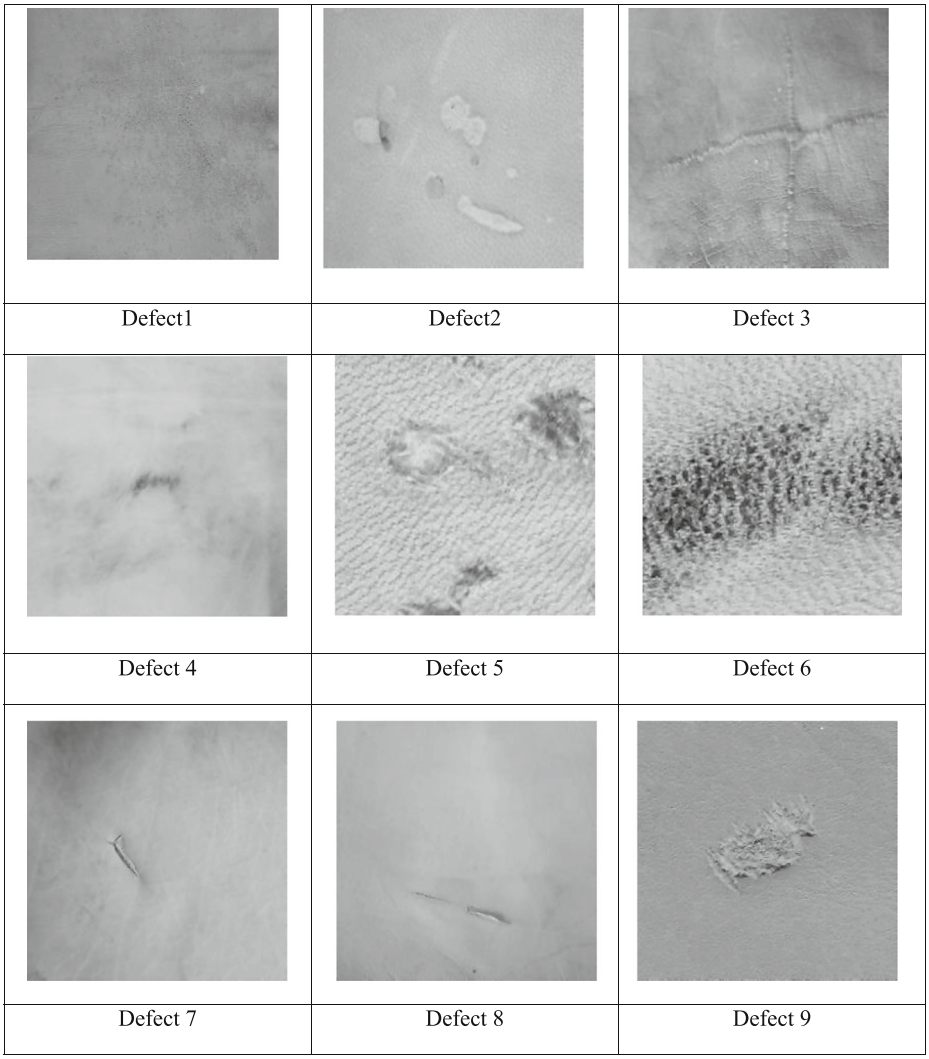

Fig. 4 Enhanced Image preprocessed using Wiener filter

function [Eq. 7] describes the texture property of the leather image and converges on the desired defect boundary. Therefore FCPSO method converged faster than conventional PSO. [Table 2]. Initial parameters of the PSO, DPSO, FODPSO and proposed FCPSO were given in Table 1.

3.1 Time complexity

Since computation time is one of the most important and critical factors for industrial leather defect application, this aspect has been given due importance in this study. With regard to CPU processing time for finding optimized threshold, it has been proven in the literature that PSO require less time when compared to GA and BF [54]. Hence, CPU time of PSO, DPSO,FODPSO and FCPSO were only compared. From Table 2, it can be

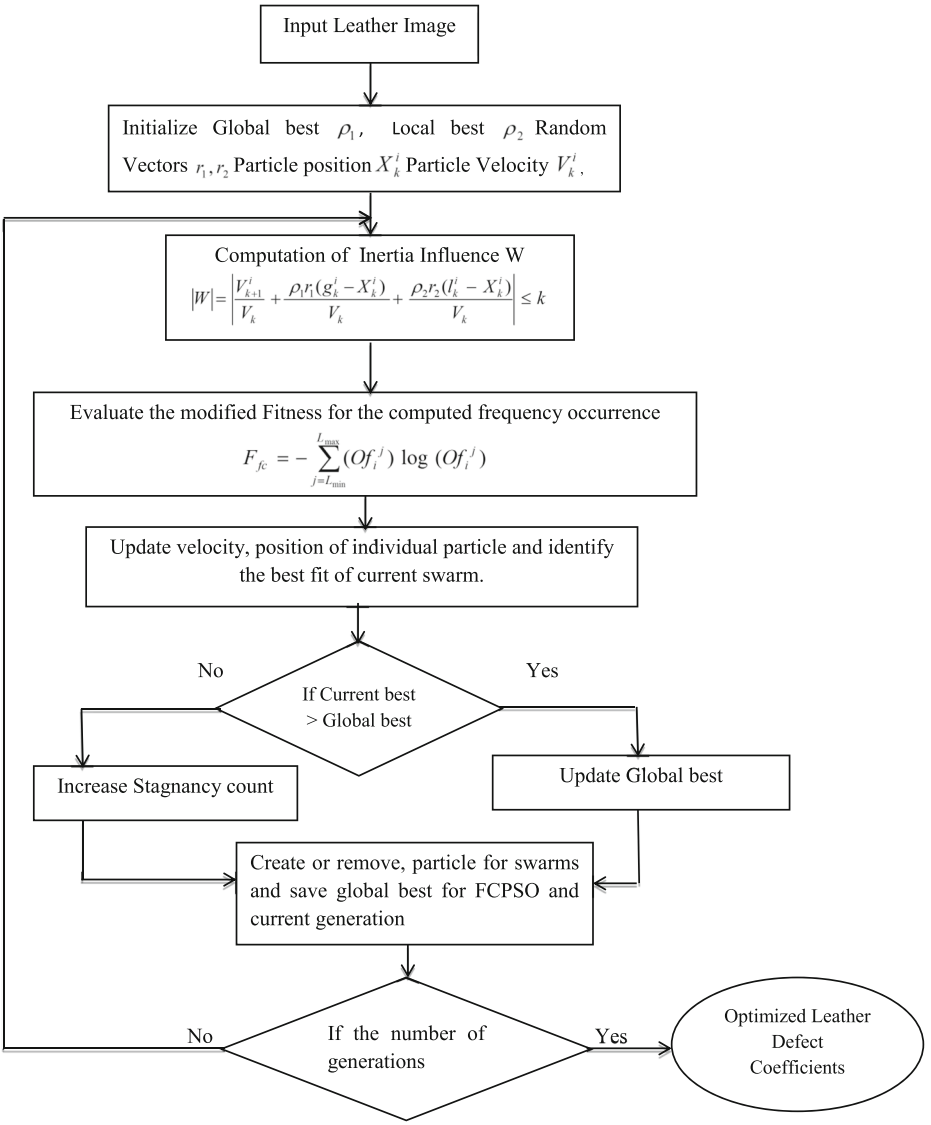

Fig. 5 Proposed FCPSO Algorithm

observed that the average computation time for PSO based segmentation algorithms varied from 0.33 to 0.45 s whereas FCPSO based segmentation algorithm varies from 0.22 to 0.35 s. From visual perspective, the quality of the segmented image using FCPSO was found to be superior for different defective images. Also, it can be observed that the computational time for random particle initialized PSO based segmentation algorithms were higher than the proposed method. This happens because the drifting behavior of particles around false solutions was avoided by initializing the particles using the entropy values which describe the texture property of the leather image. PSO having a fixed

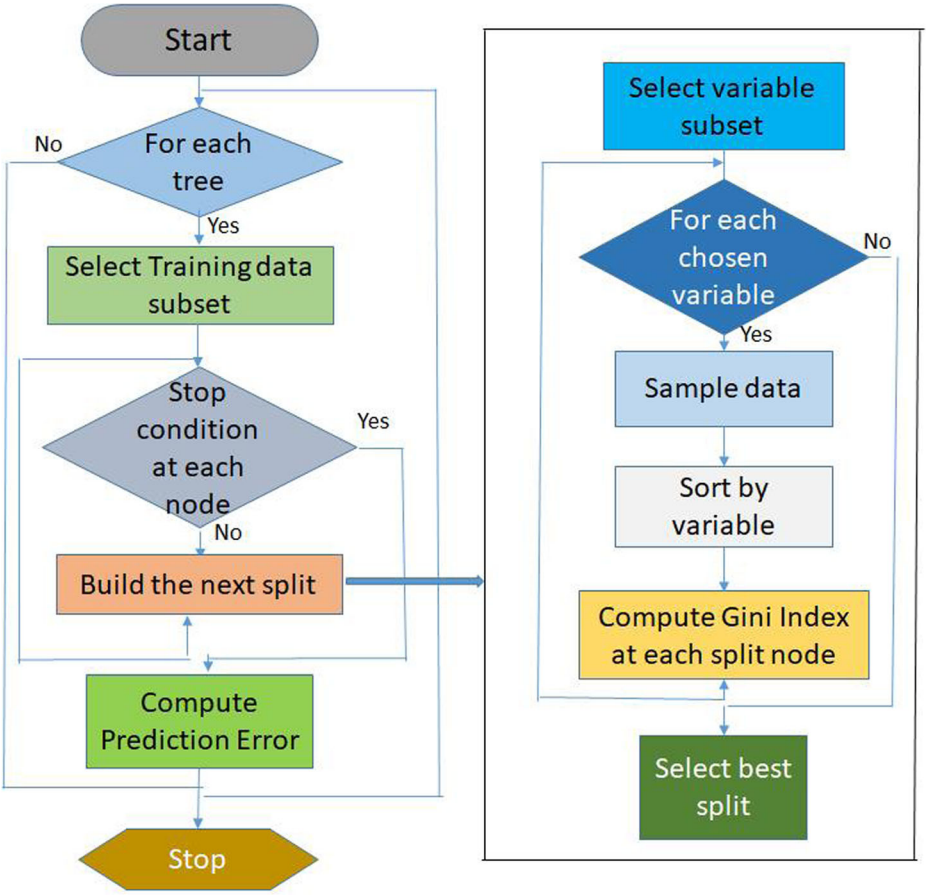

Fig. 6 Flow chart of random forest algorithm

population (100 particles) ends up evaluating 100 solutions within the same swarm resulting in higher computation time. In comparison, FCPSO consisting of smaller swarms between 2 and 6 of 10 and 50 particles each, led to faster convergences towards optimal threshold values. The least computation time was achieved for FCPSO based segmentation using selective band entropy varied from 0.28 s to 0.33 s.

The segmented output of leather images using Fast Convergence Particle Swarm Optimization (FCPSO) method for the different types of defects are shown in Fig. 8. Correlation (R = 0.84) of the proposed FCPSO segmented area with the experts ground truth was observed to be high (Fig. 9).

3.2 Stability analysis

Bio-inspired evolutionary methods [49] are known to be stochastic and random searching algorithms. The searching ability of these algorithms varies for each iteration, and the absolute results do not remain the same. To analyze the stability, standard deviation values were computed and listed in Table 3. The lower value for the standard deviation indicates the

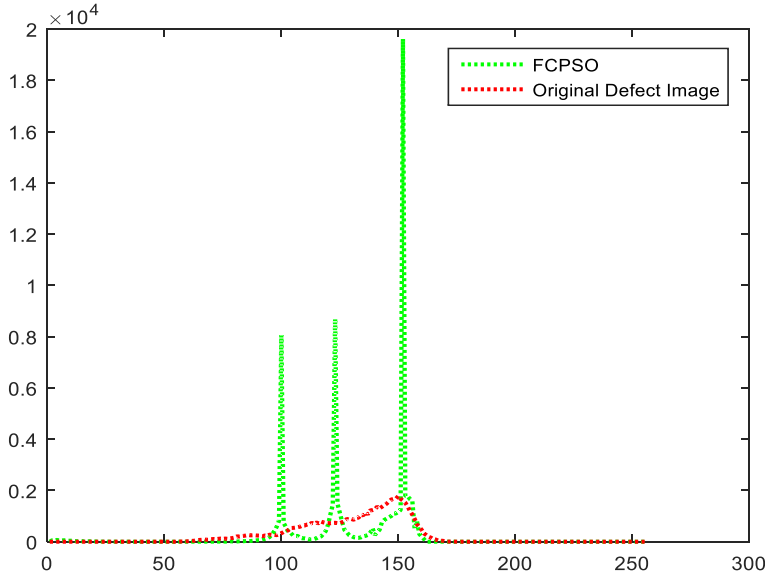

Fig. 7 Histogram distribution for leather images of the proposed FCPSO algorithm

stability of the algorithm. It can be seen from Table 3, that the proposed method was more stable than the other algorithms for all the defect images.

$$STD = \sqrt{\sum_{i=1}^{n} \frac{(\sigma_i - \mu)^2}{N}} \tag{18}$$

Where STD is the standard deviation, analyzing the best fitness value of the i^{th} run of the proposed algorithm, N is the repeated times of each algorithm ($N = 30$). From Table 1, it can be seen that FCPSO is the stable evolutionary algorithm when compared with others. FCPSO

Table 1 Initial parameters of the PSO, DPSO, FODPSO and proposed FCPSO

Parameter	Conventional PSO	DPSO (Sec)	FODPSO (Sec)	Proposed FCPSO
Num of Iterations	10	10	10	8
Population	150	50	50	40
ρ2	1.5	1.5	1.5	1.5
ρ2	1.5	1.5	1.5	1.5
W	1.2	1.2	1.2	Modified in every iteration
Vmax	2	2	2	2
Vmin	−2	−2	−2	-2
X max	255	255	255	255
X min	0	0	0	0
Min population	–	10	10	10
Max population	–	50	50	40
Num of swarms	–	4	4	4
Min swarms	–	2	2	2
Max swarms	–	6	6	6
Stagnancy	–	10	10	10
Fractional coefficient	–	–	0.75	

Table 2 Average execution time of different segmentation methods using conventional PSO with the proposed FCPSO

Test image	Conventional PSO	DPSO (Sec)	FODPSO (Sec)	Proposed FCPSO
Defect 1	0.4235	0.4382	0.3871	0.3143
Defect 2	0.3895	0.4127	0.4044	0.2715
Defect 3	0.4016	0.4112	0.3661	0.2452
Defect 4	0.4212	0.4231	0.4038	0.5501
Defect 5	0.3899	0.3879	0.3544	0.2471
Defect 6	0.3987	0.3672	0.3298	0.2712
Defect 7	0.3478	0.3321	0.3123	0.2216
Defect 8	0.4122	0.3468	0.3123	0.2421
Defect 9	0.3812	0.3912	0.3313	0.2502

based segmentation is able to converge in approximately the same amount of time, regardless of the defect image and initial condition of the particles.

Performance analysis on segmented image was further validated using quality measures Dice index, Structural similarity index (SSIM), Edge-based structural similarity index (ESSIM), structural content (SC), Normalized correlation coefficient (NK), average difference (AD), Overlap Error (OE), Area Error Rate (AER) and Zijdenbos Similarity index (ZSI) and the results are set out in Tables 4 and 5.

Similarity index (ZSI) was above 0.8 and error rates (AER, OE) were found to be 0.2. Edge-based structural similarity index (ESSIM), Normalized correlation coefficient (NK), Overlap Error (OE), Structural content (SC), Structural similarity index (SSIM) were found to be above 0.9 and Average difference (AD) was found to be around 0.05. Thus, the performance measures results that the proposed FCPSO algorithm could be used for segmentation of leather defects.

Feature extraction was carried out with the FCPSO segmented images. Texture features extracted act as predictor coefficients to identify the leather surface defects and provide vital information reflecting the coarseness, smoothness, contrast, homogeneity and randomness of pixel distribution. The mean and standard deviation values of the extracted GLCM feature are shown in Table 6.

Figure 10 shows the correlation coefficients of the forty feature variables used in this study. The correlation plot shows the strength and direction of the feature variables. Blue color indicates the variable to be positively correlated whereas red color indicates the variable to be negatively correlated and the strength of the variable ranges from +1 to −1 and appear as large circle to small circle. The diagonal elements show how each feature variable is well positively correlated with itself. The key relationship is the feature variable correlation with the target class ‘y’ (non-defective or defective) is shown in the last row. It can be observed that the features Autocorrelation - Average (V1), Cluster shade - Average (V5), Maximum probability-Average (V10), Sum of square (variance) - Average (V11), Sum average- Average (V12), Sum variance- Average (V13), Information measure of correlation (1) - Average (V17), Information measure of correlation (2) - Average (V18), Correlation – Range (V23), Cluster prominence – Range (V24), Cluster Shade – Range (V25), Sum of square (variance) - Range (V31), Sum average – Range (V32) and Information measure of correlation (1) - Range (V37) were weakly correlated with the target variable. To further validate, all the extracted forty features were subjected to t-test to determine the significant features which provide better classification of good and defective leathers. T-test shows if the feature value is statistically

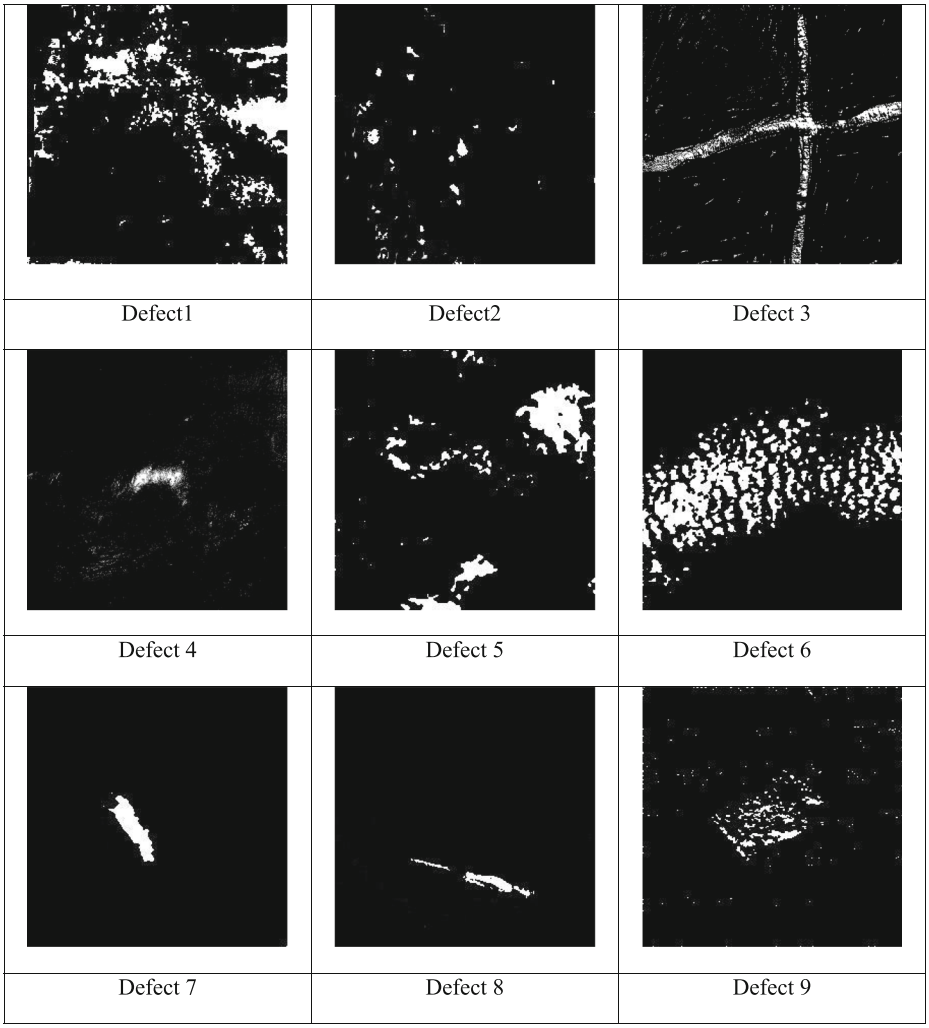

Fig. 8 FCPSO segmented output for different leather defects

significant to discriminate the non-defective and defective target value. Hence, based on correlation coefficient value and p value of t test, 24 optimal features were selected from 40 Haralick's GLCM texture features and is shown in Fig. 11. It can be clearly seen that all the selected 24 features have good discriminating ability to categorize the defective and non-defective target class. Good leather surface had a very smooth texture and was characterized with high values for feature variables such as Homogeneity, Inverse difference normalized (INN)–Average, Inverse difference moment normalized - Average and low values for the other features. While images of defective regions showed porous patches with rough and coarse texture, which were characterized by high values of Contrast, Dissimilarity, Entropy, etc.. Some of the defects visually seemed to have smooth texture but had variable intensity patches, and the texture features reflected good discrimination for these defects also.

The correlation plot (Fig.12) also shows that all the selected 24 co-occurrence features were well correlated with target class variable while the feature variables namely Homogeneity,

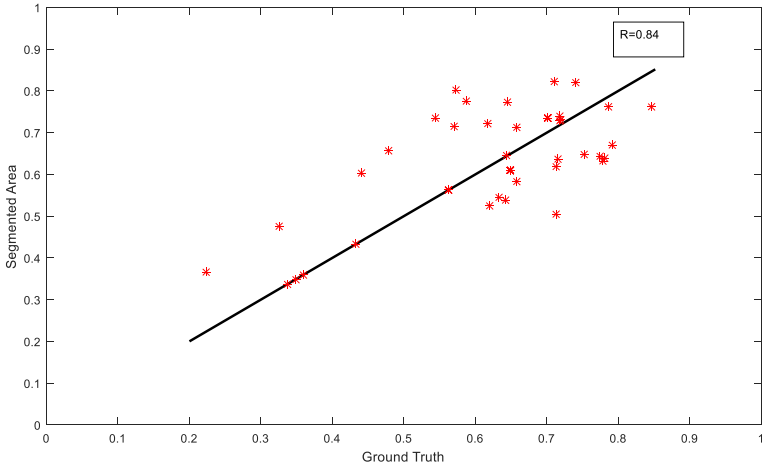

Fig. 9 Correlation Plot of Ground Truth vs proposed FCPSO segmented area

Inverse difference normalized (INN) – Average and Inverse difference moment normalized - Average found to be negatively correlated with the response variable.

In this work, performance of different classifiers such as MLP, Decision Tree, SVM, Naïve Bayes, KNN [51] and Random Forest classifiers with two classes to classify the leather surface images as the defective or non-defective class were shown in Fig.13. Initially all the extracted GLCM (40 features) were given for classification. The performance measures such as accuracy (86.11%), precision (88%), recall (86%) and F1 score (84%) of random Forest classifier significantly outperform all the other classifiers. Discriminant feature vector obtained from t-test and correlation approaches described earlier was given as input data to all the classifiers. As seen in Fig. 14, highest accuracy of 88.8% was achieved using SVM and radom forest classification. The classification accuracy for Decision Tree, MLP classifier was found to be 83.33% and 77% using Naïve Bayes classifier. Performance of Random Forest was found to be highest both before and after feature selection and hence further parameter optimization was carried out.

Random forest classifier was set for training with 250 trees, each tree was constructed (Fig. 6) considering 4 random features and training plot (Fig. 15) showed that after 50 trees, it fluctuates a bit but there was not much change in terms of error. Out-of-Bag error indicates the unbiased estimate of the classification error as trees are added to the forest and was found to be 7.2%. Information measure of correlation (2) - Range (Feature no. V21) was found to be the most important variable in terms of “Mean DecreaseGini” as well as “Mean Decrease Accuracy” The rest of the feature variables that had the greatest impact in the classification model were indicated in Fig. 15. Various combinations of reduced feature set training and testing were given as input and confusion matrix is shown in Table 7. The overall average accuracy of the random forest classifier was found to be 88.64% with 95% sensitivity, 70% specificity, 91% precision and F-score of 93%. Sensitivity is the probability that the classifier correctly classifies the defective leather as defective. Specificity is the probability that the classifier correctly classifies the good leather as normal. Due to the inherent nature of leather texture, the prominent grain pattern in good leather regions might be misread as defective regions. Hence, the specificity of the classifier is less and this may also be due to less number of non-defective samples in the set. The area under the ROC curves of random forest classifier

Table 3 Average ± STD fitness values of the proposed FCPSO and the different methods for different test cases

Test image	Proposed FCPSO	FODPSO	DPSO	PSO	GA
Defect 1	2837.7074 ± 0.0110	2837.7187 ± 0.0398	2837.7517 ± 0.2021	2837.7222 ± 0.0096	2837.7154 ± 0.0116
Defect 2	2064.2036 ± 0.0191	2064.1184 ± 0.0490	2064.2108 ± 0.0625	2064.1688 ± 0.2334	2064.0187 ± 0.3661
Defect 3	3233.3301 ± 0.1217	3232.9333 ± 0.1730	3233.4363 ± 0.9627	3232.0383 ± 2.5446	3231.7957 ± 2.4141
Defect 4	1769.1929 ± 0.0426	1769.0429 ± 0.3526	1777.2821 ± 1.2213	1765.7289 ± 2.6228	1762.6263 ± 3.2022
Defect 5	2341.3150 ± 0.1000	2341.3951 ± 0.3300	2341.3951 ± 0.0026	2341.3951 ± 0.030	2252.3164 ± 1.3171

Table 4 Performance analysis on the segmented image using the proposed FCPSO agorithm

	Dice index	SSIM	ESSIM	SC	NK
Defect 1	0.9967	0.9074	0.9978	0.9988	1.0000
Defect 2	0.9962	0.9067	0.8977	0.9840	0.9964
Defect 3	0.9967	0.9057	0.9177	0.9940	0.9953
Defect 4	0.9960	0.9052	0.9377	0.9816	0.9945
Defect 5	0.9778	0.9254	0.9232	0.9787	0.9967
Defect 6	0.9567	0.9143	0.9342	0.9687	0.9978
Defect 7	0.9596	0.9021	0.9223	0.9878	0.9934
Defect 8	0.9921	0.9045	0.8912	0.9341	0.9876
Defect 9	0.9446	0.9032	0.9443	0.9458	0.9911

trained with features selected from GLCM (Fig. 16) showed higher Az value of 0.883 closer to the top left corner.

3.3 Performance evaluation using confusion matrix

Validation was done with unseen dataset (test samples) to evaluate the ability of the classifier to discriminate the defective from non-defective leather images. The performance of the classification in leather images using Random Forest is measured in terms of Accuracy, Sensitivity, Specificity, and Precision /Positive Predictive Value (PPV), Recall / Negative Predictive Value (NPV) and F score that are often computed from a confusion matrix. There are two possible predicted classes: "present" and "absent" in the confusion matrix. For example, "present" would mean the leather to be defective and "absent" would mean the leather does not have the defect. The definitions of TP, TN, FP, and FN are as follows (Eq. 19,20,21,22,23,24,25):

- **True positives (TP):** Defective leather frames correctly classified as defects.
- **True negatives (TN):**Good leather frames correctly classified as good
- **False positives (FP):** Good leather frame wrongly classified as defective.
- **False negatives (FN):** Defective leather frame wrongly classified as good.

$$\text{Accuracy} = \frac{\text{TP} + \text{TN}}{\text{TP} + \text{FP} + \quad \text{FN} + \text{TN}} \tag{19}$$

Table 5 Quality measures of the proposed FCPSO algorithm

Defect	AD	ZSI	AER	OE
Defect 1	0.0160	0.7980	0.2119	0.2561
Defect 2	0.0635	0.8356	0.2009	0.2103
Defect 3	0.0390	0.7804	0.2131	0.2312
Defect 4	0.0687	0.8323	0.1967	0.2201
Defect 5	0.0342	0.7945	0.2215	0.2101
Defect 6	0.0422	0.8034	0.2212	0.1898
Defect 7	0.0456	0.8143	0.2123	0.2154
Defect 8	0.0676	0.7803	0.1855	0.2245
Defect 9	0.0551	0.7795	0.2491	0.2435

Table 6 Mean and standard deviation values of the extracted features

Feature No.	Feature	Mean and standard deviation feature values		*p* value
		Non Defective group	Defective group	
F1	Autocorrelation - Average	22.97 ± 2.306	23.77 ± 4.994	0.490
F2	Contrast- Average	0.047 ± 0.032	0.009 ± 0.037	<0.005
F3	Correlation- Average	0.626 ± 0.217	0.712 ± 0.092	0.010
F4	Cluster prominence- Average	0.707 ± 0.600	1.231 ± 0.761	0.005
F5	Cluster shade - Average	−0.195 ± 0.354	−0.163 ± 0.361	0.731
F6	Dissimilarity- Average	0.047 ± 0.032	0.091 ± 0.037	<0.005
F7	Energy - Average	0.730 ± 0.221	0.585 ± 0.167	0.002
F8	Entropy- Average	0.511 ± 0.381	0.819 ± 0.277	<0.005
F9	Homogeneity- Average	0.976 ± 0.016	0.954 ± 0.018	<0.005
F10	Maximum probability- Average	0.815 ± 0.168	0.713 ± 0.149	0.010
F11	Sum of square (variance) - Average	22.852 ± 2.284	23.670 ± 4.979	0.478
F12	Sum average- Average	9.554 ± 0.511	9.675 ± 0.987	0.600
F13	Sum variance- Average	83.414 ± 14.308	81.231 ± 19.170	0.637
F14	Sum entropy- Average	0.479 ± 0.359	0.756 ± 0.254	<0.005
F15	Difference variance- Average	0.047 ± 0.032	0.091 ± 0.037	<0.005
F16	Difference entropy- Average	0.174 ± 0.107	0.294 ± 0.086	<0.005
F17	Information measure of correlation (1) - Average	−0.420 ± 0.170	−0.451 ± 0.090	0.280
F18	Information measure of correlation (2) - Average	0.453 ± 0.276	0.598 ± 0.128	0.001
F19	Inverse difference normalized (INN) - Average	0.994 ± 0.003	0.989 ± 0.004	<0.005
F20	Inverse difference moment normalized - Average	0.999 ± 0.0005	0.998 ± 0.0005	<0.005
F21	Autocorrelation – Range	0.010 ± 0.007	0.025 ± 0.013	<0.005
F22	Contrast – Range	0.024 ± 0.018	0.053 ± 0.026	<0.005
F23	Correlation – Range	0.158 ± 0.067	0.161 ± 0.052	0.844
F24	Cluster prominence – Range	0.075 ± 0.053	0.198 ± 0.158	0.001
F25	Cluster shade – Range	0.034 ± 0.027	0.052 ± 0.033	0.038
F26	Dissimilarity – Range	0.024 ± 0.018	0.053 ± 0.026	<0.005
F27	Energy – Range	0.020 ± 0.014	0.041 ± 0.017	<0.005
F28	Entropy – Range	0.057 ± 0.042	0.108 ± 0.046	<0.005
F29	Homogeneity – Range	0.012 ± 0.009	0.026 ± 0.013	<0.005
F30	Maximum probability – Range	0.012 ± 0.008	0.026 ± 0.0132	<0.005
F31	Sum of square (variance) - Range	0.011 ± 0.012	0.012 ± 0.008	0.892
F32	Sum average – Range	0.0006 ± 0.0005	0.0005 ± 0.0004	0.349
F33	Sum variance – Range	0.710 ± 0.511	1.326 ± 0.585	<0.005
F34	Sum entropy – Range	0.040 ± 0.030	0.071 ± 0.028	<0.005
F35	Difference variance – Range	0.024 ± 0.018	0.053 ± 0.026	<0.005
F36	Difference entropy – Range	0.065 ± 0.042	0.115 ± 0.039	<0.00
F37	Information measure of correlation (1) - Range	0.177 ± 0.030	0.204 ± 0.040	0.008
F38	Information measure of correlation (2) - Range	0.067 ± 0.023	0.109 ± 0.037	<0.005
F39	Inverse difference normalized (INN) – Range	0.002 ± 0.002	0.005 ± 0.002	<0.005
F40	Inverse difference moment normalized – Range	0.0003 ± 0.0002	0.0008 ± 0.0004	<0.005

$$\text{Sensitivity} = \frac{\text{TP}}{\text{TP} + \text{FN}} \tag{20}$$

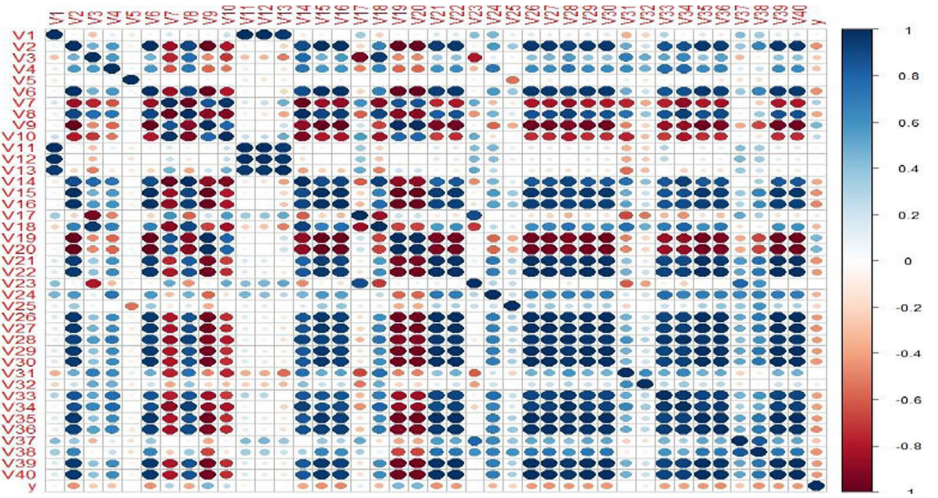

Fig. 10 Correlation plot for GLCM features – before Feature Selection

$$\text{Specificity} = \frac{\text{TN}}{\text{TN} + \text{FP}} \tag{21}$$

$$\text{Precision or PPV} = \frac{\text{TP}}{\text{TP} + \text{FP}} \tag{22}$$

$$\text{Recall or NPV} = \frac{\text{TN}}{\text{TN} + \text{FN}} \tag{23}$$

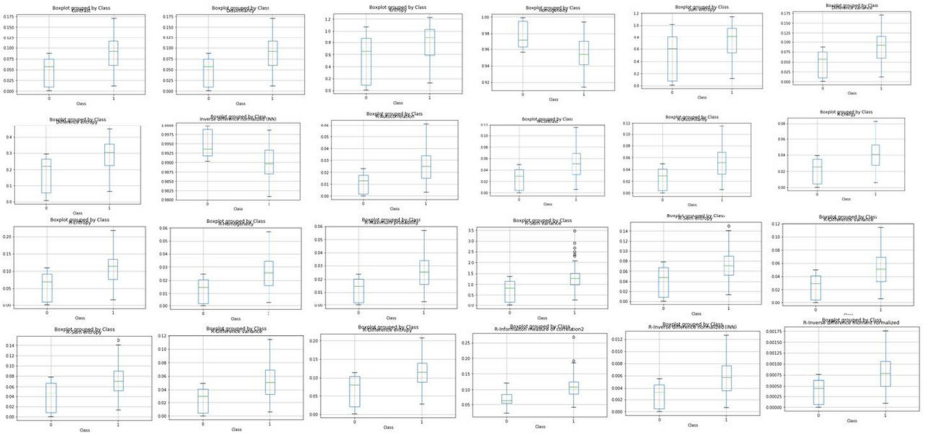

Fig. 11 Optimal texture features selected for leather defect Classification

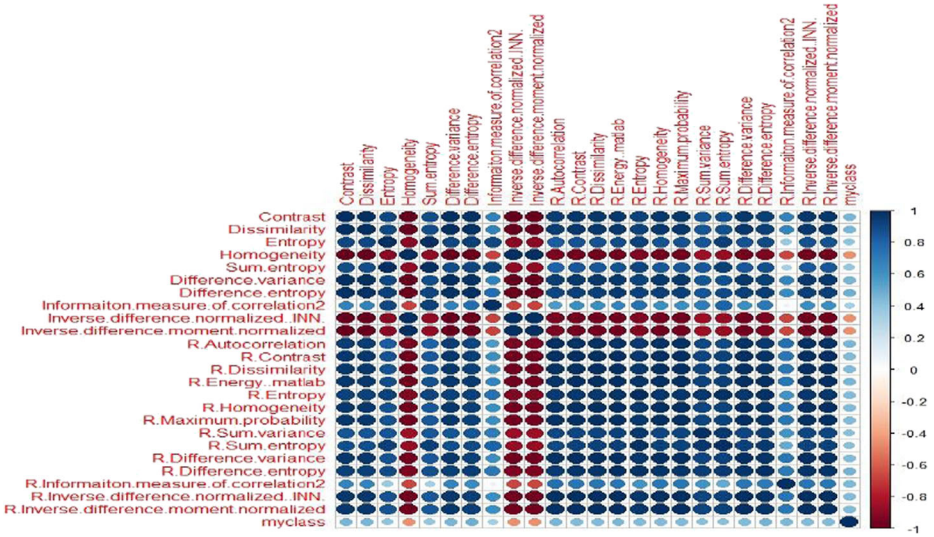

Fig. 12 Correlation plot for Haralick Co-occurrence - selected features

$$F1Score = 2*(Recall*Precision)/(Recall + Precision) \tag{24}$$

Also, Matthews correlation coefficient (Mcc) [Mathew B 1975], a measure of the quality of binary (two class) classifications expressed as

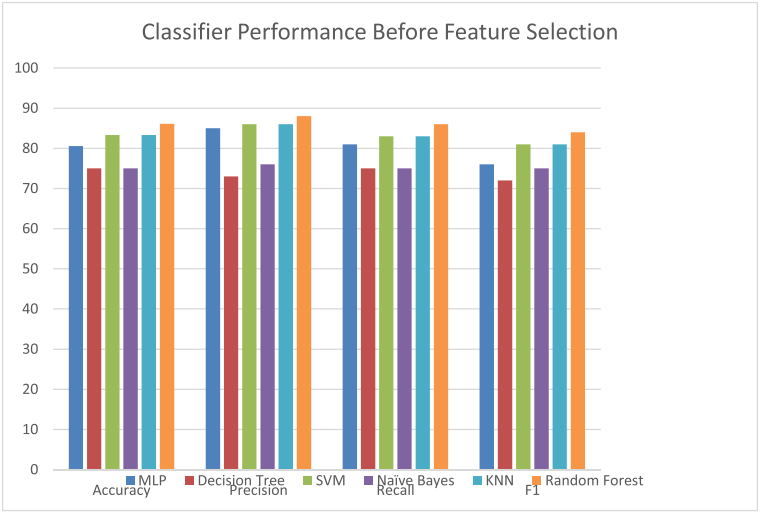

Fig. 13 Classifiers performance before feature selection

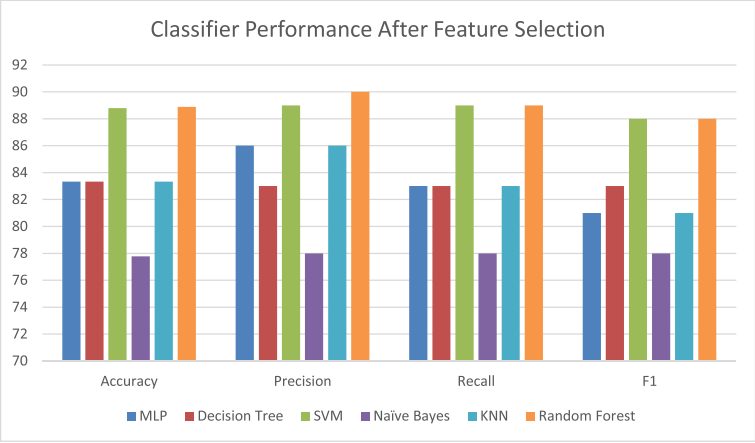

Fig. 14 Classifiers performance after feature selection

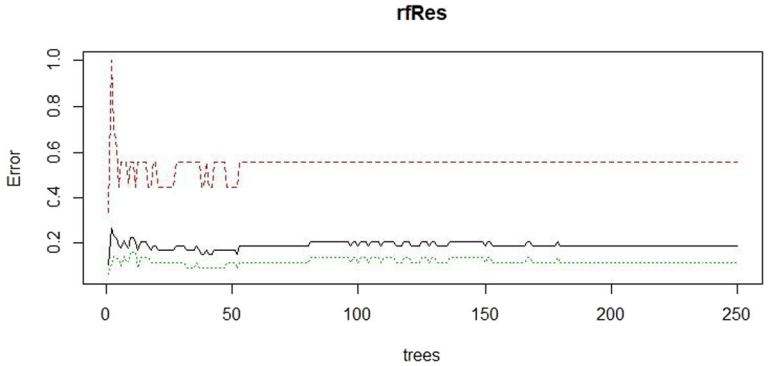

Fig. 15 Out of bag error rate for random forest classifier

Table 7 Confusion matrix for random forest trained using optimal features GLCM

TN	FP	FN	TP	Accuracy	Error	TPR	TNR	Precision	F1-score
4	3	2	27	86.11	13.89	0.93	0.57	0.90	0.92
6	5	1	26	84.21	15.79	0.96	0.55	0.84	0.90
5	2	2	26	88.57	11.43	0.93	0.71	0.93	0.93
4	5	2	25	80.56	19.44	0.93	0.44	0.83	0.88
9	1	0	26	97.22	2.78	1.00	0.90	0.96	0.98
6	1	1	28	94.44	5.56	0.97	0.86	0.97	0.97
6	2	3	25	86.11	13.89	0.89	0.75	0.93	0.91
6	4	1	25	86.11	13.89	0.96	0.60	0.86	0.91
5	1	2	28	91.67	8.33	0.93	0.83	0.97	0.95
7	3	1	25	88.89	11.11	0.96	0.70	0.89	0.93
Average				88.64	11.36	0.95	0.70	0.91	0.93

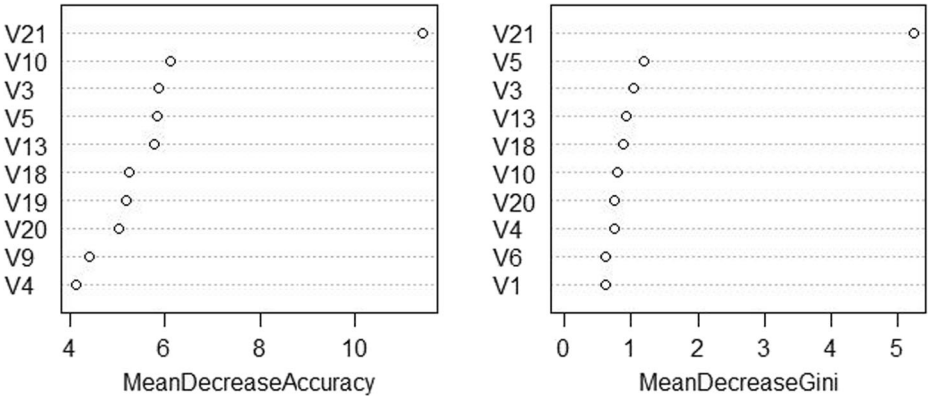

Fig. 16 Feature variable importance plot

$$M_{cc} = \frac{(TP*TN)-(FP*FN)}{\sqrt{(TP+FP)}*(TP+FN)*(TN+FP)*(TN+FN)} \tag{25}$$

Higher value of Mcc closer to +1 value represents a perfect prediction, whereas 0 represents an average random prediction and − 1 indicates an inverse prediction.

4 Conclusion

In this study, an automated leather defect detection was developed for detecting leather surface defects. The main contribution of this study lies on the industrial leather image acquisition system. An automatic Fast Convergence Particle Swarm optimization segmentation algorithm to segment the textures into homogenous (normal) and non-homogenous (defective) regions has been developed using modified inertia influence along with the new fitness function for faster convergence of particles. FCPSO segmentation results were compared with conventional PSO and other PSO variants algorithms such as DPSO, FODPSO and was found to be efficient for various leather defect images. GLCM texture features from the segmented leather were extracted. Most prominent features for automatic leather defects were selected using correlation coefficient and t-test. Extracted features were given as input to different supervised classifiers namely Neural Network (NN), Decision Tree (DT), SVM, Naïve Bayes, KNN and Random Forest (RF) were employed to classify defective and normal regions of the leather image. Results obtained concluded that, proposed FCPSO along with Random Forest algorithm using optimum feature set had good discrimination defective and non-defective leather and led to better classification accuracy 88.64% with Az and F- value of 0.883 and 0.93 respectively. The proposed system solved problems of manual segmentation of leather defects and can be used for automatic leather defect detection in leather industry.

Acknowledgments The authors acknowledge the financial support from CSIR, New Delhi under the Supra Institutional Project S&T Revolution in Leather with a Green Touch (STRAIT) communication no. A/2018/LPT/CSC0201/1275.

Appendix

Derivation of Haralick's texture features from grey level co-occurrence matrix

P(i,j) is (i,j) th entry in normalized GLCM; $P_x(i)$ is ith entry in the marginal probability matrix obtained by summing the rows of P(i,j); $P_x(i)= \sum_{j=1}^{G} P(i, j)$; $P_y(j)$ is jth entry in the marginal probability matrix obtained by summing the columns of P(i,j); $P_y(j)=\sum_{j=1}^{G} P(i, j)$; G is number of gray levels in quantized image. μ_x, μ_y,$\sigma_i\sigma_j$ are the means and standard deviation of p_x and $p_{y,}$ respectively.

No.	Feature name	Equation	Description
1	Autocorrelation	$\sum_{i,j=1}^{N} (ij)\mathrm{P}(i, j)$	Returns probability occurrence of the specific a pixel
2	Contrast	$\sum_{i,j=1}^{N} \mathrm{P}(i, j)(i, j)^2$	Returns the local variation boundary of the gray levels in a texture
3	Correlation	$\sum_{i,j=1}^{N} (i-_i)(i, _j)\mathrm{P}(i, j)/_{ij}$	Returns the probability occurrence of the specific pixel pair
4	Cluster prominence	$\sum_{i,j=1}^{N} (i + j-_x-_y)^4\mathrm{P}(i, j)$	Measures the skewness of the matrix (asymmetry)
5	Cluster shade	$\sum_{i,j=1}^{N} (i + j-_x-_y)^3\mathrm{P}(i, j)$	Measures the skewness of the GLCM (asymmetry)
6	Dissimilarity	$\sum_{i,j=1}^{N} \lvert i-j\rvert P(i, j)$	Returns linear local variation boundary of the gray levels in a texture
7	Energy (uniformity)	$\sum_{i,j=1}^{N} P(i, j)^2$	Returns the sum of squared elements in the GLCM.
8	Entropy	$-\sum_{i,j=1}^{N} P(i, j)log(i, j)$	Returns the degree of randomness and complexity of a texture
9	Homogeneity	$\sum_{i,j=1}^{N} \frac{\mathrm{P}(i,j)}{1+\lvert i-j\rvert}$	Returns the distribution consistency of the GLCM elements
10	Maximum probability	$max_{i,j}\mathrm{P}(i, j)$	Returns the largest *P(i,j)* value found within the window
11	Sum of square (variance)	$\sum_{i,j=1}^{N} (i-)^2\mathrm{P}(i, j)$	Measures the dispersion of the values around the mean
12	Sum average	$\sum_{i=0}^{2G} iP_{x+y}$	Measures the mean value of P_x and P_y
13	Sum variance	$\sum_{i=1}^{2G} (i-(\mathrm{sum}\ entropy))^2 P_{x+y}(i)$	Measures the variance of sum entropy
14	Sum entropy	$\sum_{i=0}^{2G} P_{x+y}(i)\log\left(P_{x+y}(i)\right)$	Measures the sum of P_x and $P_y$entropy
15	Difference variance	$VarianceP_{(x+y)}$	Measures the variance difference between two values
16	Difference entropy	$-\sum_{i=0}^{G} P_{x-y}(i)log\left(P_{x-y}(i)\right)$	Measures the difference of P_x and $P_y$entropy
17	Information measure of correlation (1)	$\frac{HXY-HXY1}{\max(HX,HY)}$	Measures the linear dependency of g ray levels on those of neighboring pixels.
18	Information measure of correlation (2)	$(1-\exp[-2(\mathrm{HXY2}-\mathrm{HXY})])^{0.5}$	Measures the linear dependency of gray levels on those of neighboring pixels.
19	Inverse difference normalized (INN)	$\sum_{i,j=1}^{G} \frac{1}{1+\lvert i-j\rvert^2/G^2} P(i, j)$	Returns the linear normalized distribution consistency of the GLCM elements

No.	Feature name	Equation	Description
20	Inverse difference moment normalized	$\sum_{i,j=1}^{G} \frac{1}{1+(i-j)^2/G^2} P(i,j)$	Returns the normalized distribution consistency of the GLCM elements

References

1. Ahmed N, Natarajan T, Rao KR (1974) Discrete cosine transform. IEEE Trans Comput 23:90–93
2. Alkan A, Tuncer SA, Gunay A (2014) Comparative MR image analysis for thyroid nodule detection and quantification. Measurement 47:861–868
3. Anil KJ, Mihran T (1998) Texture analysis. World Scientific Publishing Co, The Handbook of Pattern Recognition and Computer Vision, pp 207–248
4. Attila L, Dmitry C (1991) Knowledge-based Line-correction rules in a machine vision system for the Leather Industry. Engineering Applications of Artificial Intelligence 4:433–438
5. Branca A, Attolico G, Distante A (1996) Multiscale data analysis for leather defect detection. Proc. SPIE 2908, machine vision applications, architectures, and systems. Integration.:97–108
6. Branca A, Abbate MG, Lovergine FP, Attolico G, Distante A (1997a) Leather inspection through singularities detection using wavelet transforms. International Conference on Image Analysis and Processing 2:584–592
7. Branca A, Lovergine FP, Attolico G, Distante A (1997b) Defect detection on leather by oriented singularities. International Conference on Computer Analysis of Images and Patterns 1296:223–230
8. Breiman L (2001) Random forests. Mach Learn 45:5–32
9. M. Bruder (June 2019) For the qualification of leather, you need a human! Is that really the case?," Proceedings of the XXXV International Union of Leather Technologists and Chemists Societies (IULTCS), PG. 93.
10. Cao L, Bao P, Shi Z (2008) The strongest schema learning GA and its application to multilevel thresholding. Image Vis Comput 146:387–390
11. Chang J-F, et al. (2005) A parallel particle swarm optimization algorithm with communication strategies. Journal of Information Science and Engineering.
12. Chris, C.B., Peter J. H., Wayne, P.P., Michael, P.H., Richard, P.G. (1996) Sheep-pelt grading using laser scanning and pattern recognition. Proc. SPIE 2908, Machine Vision Applications, Architectures, and Systems Integration, 33, https://doi.org/10.1117/12.257274.
13. Deng, J.; Dong, W.; Socher, R.; Li, L.J.; Li, K.; Li, F.-F. (2009) ImageNet: a large-scale hierarchical image database. In Proceedings of the IEEE Conference on Computer Vision and Pattern Recognition (CVPR), Miami, FL, USA, 20–25 June; pp. 248–255.
14. Tabernik Domen, Sela Samo, Skvarc Jure, Skocaj Danijel, Segmentation-based deep-learning approach for surface-defect detection, J Intell Manuf, Vol.31, no. 3, pg. 759–776, 2020.
15. Dongping Tian EFPSO (2018) An effective fuzzy particle swarm optimization and its applications. Journal of Information Hiding and Multimedia Signal Processing 9(6):1365–1379
16. Eberhart R, Shi Y, Kennedy J (2001) Swarm intelligence. Morgan Kaufmann, San Mateo
17. Ge, W.; Yu, Y. (2017) Borrowing treasures from the wealthy: Deep transfer learning through selective joint fine tuning. In Proceedings of the IEEE Computer Vision and Pattern Recognition (CVPR), Honolulu, HI, USA, 21–26 July 2017; pp. 1086–1095.
18. Ghamisi P, Couceiro MS, Benediktsson JL, Ferreira NMF (2012) An efficient method for segmentation of images based on fractional calculus and natural selection. Expert Syst Appl 39:12407–12417
19. Girshick, R.; Donahue, J.; Darrell, T.; Malik, J. (June 2014) Rich feature hierarchies for accurate object detection and semantic segmentation. In Proceedings of the IEEE Conference on Computer Vision and Pattern Recognition (CVPR), Columbus, OH, USA, 23–28 ; pp. 580–587.
20. Hammouche K, Diaf M, Siarry P (2008) A multilevel automatic thresholding method based on a genetic algorithm for a fast image segmentation. Computer Vision Image Understanding 109:163–175
21. Haralick RM, Shanmugam K, Dinstein I (1973) Textural features for image classification. IEEE Transactions on systems, man, and cybernetics 6:610–621
22. He, F., Wang, W., Chen, Z. (2006a). Automatic defects detection based on adaptive wavelet packets for leather manufacture. In Technology and Innovation Conference (ITIC), IET International , 2024-2027.
23. He FQ, Wen W, Zi CC (2006b) Automatic visual inspection for leather manufacture. In: Key Engineering Materials, Trans Tech Publications:469–472

24. Hemerson, P., Willian P.A., Priscila, S.M., Mauro, C.P., Pereira, M.A., Jacinto, M.A.C. (2006) Defect detection in raw hide and wet blue leather. CompIMAGE, Computational Modelling of Objects Represented in Images: Fundamentals Methods and Applications, Coimbra, 355–360.
25. Hoang K, Nachimuthu A (1996) Image processing techniques for leather hide ranking in the footwear industry. Mach Vis Appl 9:119–129
26. Malathy Jawahar ,Chandra Babu N. K., Vani, K. (2014) Leather texture classification using wavelet feature extraction technique", IEEE International Conference on Computational Intelligence and Computing Research, pg. 1–4
27. Malathy Jawahar , Chandra Babu N. K., Vani, K. (2016) Compression of leather images for automatic leather grading system using Multiwavelet", IEEE International Conference on Computational Intelligence and Computing Research, pg. 1–7.
28. Malathy Jawahar , Chandra Babu N. K., Vani K. (2019) Machine Vision Inspection System For Detection of Leather Surface Defects, Journal of American Leather Chemist Association, vol.114, no.1.
29. Jiang M, Luo YP, Yang SY (2007) Stochastic convergence analysis and parameter selection of the standard particle swarm optimization algorithm. Inf Process Lett 102:8–16
30. Kaloyan K, Georgieva L (2005) Identification of leather surface defects using fuzzy logic. Proceedings of the International Conference on Computer Systems and Technologies, IIIA. 12.
31. Kasi MK, Rao JB, Sahu VK (2014) Identification of leather defects using an auto adaptive edge detection image processing algorithm. In high performance computing and applications (ICHPCA), International Conference, IEEE, 1–4.
32. Kayalvizhi M, Kavitha G, Sujatha CM, Ramakrishnan S (2015) Minkowski functionals based brain to ventricle index for analysis of AD progression in MR images. Measurement 74:103–112
33. Kennedy J, Eberhart R (1995) A new optimizer using particle swarm theory. In proceedings of the IEEE sixth international symposium on micro machine and human science:39–43
34. Khan SA, Engelbrecht AP (2012) A fuzzy particle swarm optimization algorithm for computer communication network topology design. Appl Intell 36(1):161–177
35. Kornblith, S.; Shlens, J.; Le, Q.V. (2018) Do better ImageNet models transfer better? arXiv 2018, arXiv: 1805.08974.
36. Krastev K, Georgieva L (2006) A method for leather quality determination using fuzzy neural networks. Proceedings of the International Conference on Computer Systems and Technologies
37. Kulkarni RV, Venayagamoorthy GK (2010) Bio-inspired algorithms for autonomous deployment and localization of sensor nodes. IEEE Transactions, SMC 40:663–675
38. Kwak C, Ventura JA, Sazi KT (2000) A neural network approach for defect identification and classification on leather fabric. J Intell Manuf 11:485–499
39. Kwak C, Ventura JA, Sazi KT (2001) Automated defect inspection and classification of leather fabric. Intelligent Data Analysis 5:355–370
40. LeCun, Y.; Bengio, Y.; Hinton, G. Deep learning. Nature , 521, pg. 436–444, 2015.
41. Limas Serafim, A.F. (1992) Segmentation of natural images based on multiresolution pyramids linking of the parameters of an autoregressive rotation invariant model, Application to leather defects detection. Proceedings, 11th IAPR International Conference on Pattern Recognition. Vol. III. Conference C: image, Speech and Signal Analysis, The Hague, 41–44.
42. Limas-Serafim, A.F. (1993). Natural images segmentation for patterns recognition using edges pyramids and its application to the leather defects. Industrial Electronics, Control, and Instrumentation, Proceedings of the IECON '93. International Conference on, Maui, HI, 1357–1360.
43. Liong, S.T.; Gan, Y.; Huang, Y.C.; Yuan, C.A.; Chang, H.C. (2019) Automatic defect segmentation on leather with deep learning. arXiv 2019, arXiv:1903.12139.
44. Lovergine FP, Branca A, Attolico G, Distante A (1997) Leather inspection by oriented texture analysis with a morphological approach. Proceedings of International Conference on Image Processing, Santa Barbara, CA 2:669–671
45. Maitra M, Chatterjee A (2008a) A hybrid cooperative-comprehensive learning based PSO algorithm for image segmentation using multilevel thresholding. Expert Syst Appl 34:1341–1350
46. Maitra M, Chatterjee A (2008b) A novel technique for multilevel optimal magnetic resonance brain image thresholding using bacterial foraging. Measurement 41:1124–1134
47. Mario MN, Oduvaldo V, Fusco JPA (2005) Automated system for leather inspection: the machine vision. Emerging Solutions for Future Manufacturing Systems 159:387–396
48. Mohagheghian E, James LA (2018) Optimization of hydrocarbon water alternating gas in the Norne field: application of evolutionary algorithms. Fuel 223:86–98
49. Nanni, L.; Ghidoni, S.; Brahnam, S Handcrafted vs non-handcrafted features for computer vision classification Pattern Recognit, Vol. 71, pg. 158–172, 2017.

50. Pereira, R.F.; Medeiros, C.M.; Rebouças Filho, P.P. (July 2018) Goat leather quality classification using computer vision and machine learning. In Proceedings of the 2018 International Joint Conference on Neural Networks (IJCNN), Rio de Janeiro, Brazil, 8–13; pp. 1–8.
51. Peters S, Koenig A (2007) A hybrid texture analysis system based on non-linear & oriented kernels, particle swarm optimization, and kNN vs. Support Vector Machines. 7th International Conference on Hybrid Intelligent Systems, 1–25.
52. Pölzleitner W, Niel A (1994) Automatic inspection of leather surfaces. Society of Photooptical Instrumentation Engineers 2347:50–58
53. Ren R, Hung T, Tan K.C., A generic deep-learning-based approach for automated surface inspection. IEEE Trans Cybern 48, pg. 929–940, 2017.
54. Sathya PD, Kayalvizhi R (2010a) PSO based thresholding selection procedure for image segmentation. International Journal of Computer Applications 5:39–46
55. Sathya PD, Kayalvizhi R (2010b) A new multilevel thresholding method using swarm intelligence algorithm for image segmentation. J Intell Learn Syst Appl 2:126–138
56. Sezgin M, Tasaltin R (2000) A new dichotomization technique to multilevel thresholding devoted to inspection applications. Pattern Recogn Lett 21:151–161
57. Shannon CE (1935) A mathematical theory of communication. Bell System Technical Journal 27:379–423
58. Sharon, J. Jenifa, L. Jani Anbarasi, and Benson Edwin Raj (2018) DPSO-FCM based segmentation and classification of DCM and HCM Heart Diseases." 2018 Fifth HCT Information Technology Trends (ITT). IEEE, 2018.
59. Siva S, Sindhu S, Geetha S, Kannan A (2012) Evolving optimised decision rules for intrusion detection using particle swarm paradigm. International Journal of Systems Science 43(12):2334–2350
60. Sorbal JL (2005) Leather inspection based on wavelets. Iberian conference on pattern recognition and image analysis, LNCS 3523:682–688
61. Sorwar G, Abraham A (2004) DCT based texture classification using soft computing approach. Malays J Comput Sci 17:13–23
62. Sun C, Shrivastava, A.; Singh, S.; Gupta, A. (2017) Revisiting unreasonable effectiveness of data in deep learning era. In Proceedings of the IEEE International Conference on Computer Vision (ICCV), Venice, Italy, 22–29 October 2017; pp. 843–852.
63. Teng, Zhi-Jun, et al. (September 2018) Particle swarm optimization algorithm based on dynamic acceleration factor in wireless sensor network. Journal of Information Hiding and Multimedia Signal Processing, Volume 9, Number 5
64. Villar, P., Mora, M., Gonzalez, P. A new approach for wet blue leather defect segmentation. In Ibero american Congress on Pattern Recognition, Springer Berlin Heidelberg, 2011, 591–598.
65. Wang L, Liu C (1765-1768) Tanning leather classification using an improved statistical geometrical feature method. IEEE in Machine Learning and Cybernetics, International Conference 3:2007
66. Wang Q, Liu H, Liu J, Wu T (1992) A new method for leather texture image classification. Proceedings of the IEEE International Symposium Conference in Industrial Electronics:304–307
67. Weszka JS, Dyer CR, Rosenfeld A (1976) A comparative study of texture measures for terrain classification. IEEE Transactions on Systems, Man, and Cybernetics: Systems 6:269–285
68. Woo KJ, Choo YY, Choi HH, Cho JM, Kil GS (2004) Development of leather quality discrimination system by texture analysis. TENCON Region 10 Conference:327–330
69. Xiaohui, H., Yuhui, S., Eberhart, R. (2004) Recent advances in particle swarm. IEEE Proceedings of the 2004 Congress on Evolutionary Computation, 19–23.
70. Yamille DV, Ganesh KV, Salman M, Jean-Carlos H, Ronald GH (2008) Particle swarm optimization: basic concepts variants and applications in power systems. IEEE Transactions On Evolutionary Computing:171–195
71. Yeh C, Perng DB (2005) A reference standard of defect compensation for leather transactions. Int J Adv Manuf Technol 25:1197–1204
72. Yin PY (1999) A fast scheme for optimal thresholding using genetic algorithms. Signal Process 72:85–95
73. Zweig MH, Campbell G (1993) Receiver-operating characteristic (ROC) plots: a fundamental evaluation tool in clinical medicine. Clin Chem 39:561–577

Publisher's note Springer Nature remains neutral with regard to jurisdictional claims in published maps and institutional affiliations.

Malathy Jawahar is the Principal Scientist in Leather Process Technology department of CSIR- Central Leather Research Institute and an honorary faculty of Anna University. She received B.E. and M.S. degrees in Computer Science and Engineering in 1992 and 2003, respectively from Madurai Kamaraj University and Anna University, Chennai, India. Her areas of expertise include image processing, artificial neural networks, application software development, computer aided colour matching, mathematical modeling etc. She has published 15 International journal publications and 3 copyrights. She joins the review committee for IEEE Transactions on Instrumentation and Measurement, Computers in Industry, Coloration technology journals. She is a recipient of Young Scientist Award in Asian Leather Conference Taiwan – Nov 2012 and bagged best paper awards in IEEE International Conference on Computational Intelligence and Computing Research in 2014 and 2016.

Dr. N.K. Chandra Babu is the former chief scientist of CSIR – CLRI. His area of specialization is leather science and technology. He is a recipient of Jawaharlal Nehru Memorial Award for university I rank in B.Tech and M.Tech (Leather). He also received the award for best contribution to leather Industry by All India Hides and skins Tanners and Merchants Association (AISHTMA). He received J Sinha Roy Memorial Award in Journal of Indian Leather Technologists Association for three years. He is also the recipient of the Bry Air Special Commendation award for the design of Mobile Chiller for the salt-less curing of skins and hides.

He coordinated with many Governmental agencies in coming out with policy support for the growth of Leather sector in India. He authored/edited 5 manuals and 2 book chapters. To his credit he filed 24 patents and one copyright. He has published more than 110 research articles.

Dr. K. Vani is the Professor in Department of Information Science and Technology, College of Engineering Guindy, Anna University, Chennai, India. Her area of specialization is Image Processing. She received M.E in Electronics and Communication Engg. and Ph.D (Image Processing) degrees from Anna University. She has published more than 35 research articles in International Journals. She has received IGS Best paper award for Young Scientist in 2002, Faculty Mentor Award by IBM academic initiative in 2007 and Lunar and Planetary Institute career development award given by Lunar and Planetary Science Conference, USA in 2010.

L. Jani Anbarasi received BE degree from Manonmanium Sundaranar University in 2000 and ME and Ph.D. degrees from Anna University in 2005 and 2015, respectively. Currently, she is a Assistant Professor (Sr) in VIT Chennai, India. She has 11 years of teaching experience at the graduate level. Her research interests include Cryptography, Image Processing and Medical applications. She is a professional member is ISTE, ACM bodies. She has received Best Paper awards in IEEE conferences.

Dr. S. Geetha is a Professor in School of Computing Science and Engineering, VIT University, Chennai Campus, India. She has received the B.E., and M.E., degrees in Computer Science and Engineering from Madurai Kamaraj University, India in 2000 and Anna University of Chennai, India in 2004, Ph.D. Degree from Anna University in 2011, respectively. She has rich teaching and research experience. She has published more than 100 papers in reputed International Conferences and refereed Journals. Her research interests include steganography, steganalysis, multimedia security, intrusion detection systems, malware analysis, machine learning paradigms and information forensics. She is a recipient of University Rank and Academic Topper Award in B.E. and M.E. in 2000 and 2004 respectively. She also holds the Certificate of Appreciation from IBM in 2009, 2010 for Great Mind Challenge, Mentor IBM Academic Initiative Program. She has also served as the TPC Member and Review Member for more than 30 IEEE and Springer supported international conferences apart from more than 10 peer reviewed SCI-Indexed journals. She is also the proud recipient of ASDF Best Academic Researcher Award 2013, ASDF Best Professor Award 2014, Research Award-2016 and High Performer Award – 2016, from VIT University, ISCA – Best Poster Award 2018. She serves as a Life Member in HKCBEES, ISCA, IACSIT, and IAENG.

Affiliations

Malathy Jawahar[1,2] · N. K. Chandra Babu[1,2] · K. Vani[3] · L. Jani Anbarasi[4] · S. Geetha[4]

N. K. Chandra Babu
babunkc@yahoo.com

K. Vani
vani@anna.edu

L. Jani Anbarasi
janianbarasi.l@vit.ac.in

S. Geetha
geetha.s@vit.ac.in

[1] Leather Process Technology Division, CSIR-Central Leather Research Institute, Adyar, Chennai 600020, India

[2] Department of Leather Technology, Anna University, Chennai 600 025, India

[3] Department of Information Science and Technology, Anna University, Chennai 600 025, India

[4] School of Computer Science and Engineering, Vellore Institute of Technology, Chennai Campus, Chennai 600 127, India